# Autofocusing of SAR images based on parameters estimated from the PHAF

*Vesna Popović, Igor Djurović, LJubiša Stanković, Thayananthan Thayaparan, Miloš Daković*

*Abstract*— **The local polynomial Fourier transform (LPFT) based algorithm for autofocusing SAR images has recently been proposed by the authors. It produces a well focused image of moving targets, without defocusing stationary targets or inducing undesired cross-terms. The drawback of this algorithm is its high computational burden caused by the large number of elements in the set of used chirp-rates. We propose an algorithm with decreased number of elements used for the LPFT-based SAR imaging. The product high-order ambiguity function (PHAF) is applied to estimate parameters of a radar signal. The estimated chirp-rate is used as an initial value for forming the set of chirp-rates. The proposed algorithm has significantly smaller set of chirp-rate values (tens comparing to several hundreds or thousands used in the previous algorithm version). In this manner, the calculation complexity is significantly reduced. The proposed procedure is fully automated, meaning that it follows the change of motion parameters. In addition, our procedure considers the third-order phase compensation.**

## I. Introduction

The synthetic aperture radar (SAR) is a system for obtaining high resolution radar image based on the relative angle change of the radar with respect to a target during the emission of radar signal. High resolution is achieved by coherent processing of reflected signals. The viewing angle change is produced by a radar carried on a platform moving at uniform speed and constant altitude [1]. In the case when SAR targets are stationary, the radar signal is composed of a sum of complex sinusoids. The resulting SAR images, obtained by using the 2D Fourier transform (2D FT), as a common technique for SAR imaging, are well focused [1]-[4]. However, for moving targets, the corresponding signals are linear frequency modulated (FM) [1]. Moreover, recent surveys [5], [6] have shown that higher-order phase FM signals are the appropriate models of radar returns from non-uniformly moving targets. Therefore, the 2D FT is not an adequate tool for SAR imaging of moving targets, since they can be spread in the 2D Fourier domain [5]-[8]. More sophisticated techniques should be therefore used.

In the open literature, several groups of techniques are used for focusing SAR images. One group is based on the motion compensation. The motion compensation can be performed by estimating parameters of received signal, which are related to the motion parameters of targets [1]. A widely used motion compensation technique is the nonparametric phase gradient autofocusing (PGA) algorithm [9]-[11]. The aim of the PGA is to remove higher-order coefficients induced in the phase of the SAR signal as a result of long observation time or unknown exact radar velocity. The PGA is based on averaging the estimated phase gradient along the range bins, assuming that the phase error (higher-order coefficients) is equal in each range bin [11]. Therefore, it cannot be used for moving target detection and imaging [12]. A significant work on autofocusing of SAR image in the case when defocusing is induced by unknown true velocity of sensor is done by A. Moreira [13], [14]. As an alternative, a procedure for applying the product high-order ambiguity function (PHAF) for focusing SAR images is proposed in [12]. This procedure can be utilized for detection and imaging of moving targets in some specific cases. More precisely, it is based on the assumption that in case of multi-peak PHAF, there is one or more moving targets in the observed range cell. The phase coefficients of the corresponding signal are then estimated from the PHAF, which is a very accurate, compu-

Signal Processing, Vol. 90, No. 5, May 2010.

tationally simple technique for parameter estimation of multicomponent polynomial phase signals (PPS) [15]. Estimated values are used for the signal dechirping [12]. This dechirping results in defocusing of the initially focused stationary background (targets). Moreover, it causes additional phase modulation of targets, that are in the same range bin, but with different motion parameters. In order to overcome these drawbacks, an algorithm for separating signal components corresponding to targets with different motion parameters should be applied.

As an alternative, the utilization of the time-frequency (TF) analysis for SAR imaging in case of moving targets has been intensively studied [1], [16], [17]. Some of the most common TF representations, such as the Wigner distribution (WD), produce highly concentrated signal terms, but with the drawback of appearance of undesired interference terms (cross-terms) [18], [19]. Recently, the adaptive S-method (SM) for SAR imaging has been proposed [20]. It is computationally simple and produces highly concentrated SAR images, without defocusing the targets already focused in the initial 2D FT based image or inducing undesired interference terms. However, the adaptive SM may not separate targets that are very close [21]. Recently, the linear local polynomial Fourier transform (LPFT) based technique is proposed in [22], which can focus very close targets. In addition, the LPFT-based technique is more robust to additive noise than the adaptive SM [21]. The drawback of the LPFT-based technique is high computational complexity needed for selection of chirp-rate that produces the best concentration.

In the algorithm proposed here, an adaptive set of chirp-rates is formed for each unfocused target. When one or more unfocused targets are detected in a range, the PHAF is evaluated and its maximum's position is used for the chirp-rate estimation. In each algorithm iteration, the chirp-rate of one target (or couple of targets with the same or similar motion parameters) is estimated (coarse search). Further improvement of the obtained estimate is performed by using a fine search in the region around the obtained chirp-rate from the coarse search. The fine search is performed in an interval of two frequency bins from each side of the frequency that the coarse estimate corresponds to. Number of chirp-rates corresponding to the considered interval is rather small (usually not larger than several tens) which yields a significant decrease in computational complexity with respect to the technique proposed in [22] (which requires hundreds or thousands). More importantly, the algorithm is fully automated by the proposed modification since the coarse search follows the position of the PHAF maximum which corresponds to the chirp-rate related to any motion parameters of interest. The same resolution with a predefined set can be obtained only if it covers wide range of chirp-rates, which additionally increases the calculation complexity. In addition, a procedure for the third-order phase compensation is applied in the proposed algorithm without significant increase of the calculation burden.

The paper is organized as follows. In section 2, the SAR signal model and the 2D FT are reviewed. The LPFT-based algorithm for SAR imaging, with the PHAF-based parameter estimation, is proposed in Section 3. Simulation results are given in Section 4, while the conclusions are drawn in Section 5.

## II. Signal model

The point scatterer model is assumed here for modeling radar signal [1]. The received radar signal, after some preprocessing, can be written as the sum of FM signals [1], that is:

$$q(m,n) = \sum_i \sigma_i e^{j\phi_i(m,n)}, \qquad (1)$$

where $\sigma_i$ is the reflection coefficient of the corresponding scatterer, $m$ corresponds to the number of transmitted chirp ("slow-time") and $n$ corresponds to the sample index within the chirp ("fast-time"). Form of the phase functions $\phi_i(m,n)$ depends on the type of the corresponding radar scatterer.

The radar image can be obtained by using the 2D FT as:

$$Q(m',n') =$$

$$\sum_m \sum_n q(m,n)w(m,n)e^{-j\frac{2\pi}{M}mm'-j\frac{2\pi}{N}nn'}, \quad (2)$$

where $N$ is the number of samples within one pulse, $M$ is the number of pulses in one revisit and $w(m,n)$ is the window function.

In case of stationary target in the SAR systems, $\phi_i(m,n)$ can be approximated by the first-order polynomial over $m$ and $n$ [1]. The corresponding 2D FT is:

$$Q_i(m',n') = \sigma_i W(m' - \frac{M}{2\pi}a_i^{(1)}, n' - \frac{N}{2\pi}b_i^{(1)}), \quad (3)$$

where $W$ is the 2D FT of the window function, while parameters $(a_i^{(1)}, b_i^{(1)})$ correspond to the position of the $i$th scatterer. Since the used window is usually highly concentrated in the FT domain, we can assume that stationary targets are highly concentrated around their positions in the range/cross-range domain.

Target moving with uniform velocity produces $\phi_i(m,n)$ that is the second-order polynomial along $m$, while it is the first-order polynomial along $n$ [1]. In addition, returns from non-uniformly moving targets in the SAR systems can be accurately represented with the higher-order polynomial phase FM signals along $m$ [5], [6]. Thus, for these kinds of targets, the phase function can be written as [20]:

$$\phi_i(m,n) = a_i^{(1)}m + b_i^{(1)}n + \psi_i(m,n), \quad (4)$$

where $\psi_i(m,n)$ represents the higher-order terms in the signal phase. The 2D FT can be then represented in the following form:

$$Q_i(m',n') = \sigma_i W(m' - \frac{M}{2\pi}a_i^{(1)}, n' - \frac{N}{2\pi}b_i^{(1)}) \\ *_{m'} *_{n'} FT\{e^{j\psi_i(m,n)}\}, \quad (5)$$

where $*_{m'}*_{n'}$ represents the 2D convolution, while the term $FT\{\exp(j\psi_i(m,n))\}$ causes spreading.

Recall that the essential part of the PGA [9]-[11] is averaging the estimated phase gradient along the range bins. Thus, it cannot be used for moving target focusing. Moving target focusing can be achieved, for some specific scenarios, by the technique proposed in [12], but the existence of one dominant scatterer is needed. More precisely, the SAR image, obtained by this technique, will be focused only when one target exists in range bin, or when all targets in one range bin have similar motion parameters. Otherwise, the proposed technique will fail to achieve high concentration of each target simultaneously in one range bin. Therefore, an algorithm that extracts the signals from a mixture, and separately focuses targets with different motion parameters, should be used. One such an algorithm is proposed in [22], but it is computationally demanding. A procedure for decreasing the number of calculations in this algorithm and its automation is proposed in the next section. The third-order LPFT is used here to focus the radar image of non-uniformly moving targets.

## III. An algorithm for parameters estimation and autofocusing of SAR images

### A. Local Polynomial Fourier Transform and Product High-Order Ambiguity Function

The spreading in the SAR systems commonly occurs only in the cross-range domain [1] and we perform autofocusing operations only in this domain. Consider then a discrete signal $x(m)$ representing the radar signal for a fixed range $n'$:

$$x(m) = \\ Q_0(m,n') = \sum_n q(m,n)w(m,n)e^{-j\frac{2\pi}{N}nn'}. \quad (6)$$

Suppose that there is a moving target in the corresponding range cell. The resulting radar signal can be modelled as a PPS [1], [20]:

$$x(m) = Ae^{j\sum_{p=0}^{P}\alpha_p m^p} \\ = Ae^{j(\alpha_0+\alpha_1 m+\cdots+\alpha_P m^P)}, \quad (7)$$

where $\alpha_p$ are phase coefficients, $P$ is the order of the phase polynomial, and amplitude $A$ is assumed to be constant.

The LPFT for focusing SAR images in the cross-range domain, used in [22], can be written as:

$$Q_\alpha(m') = \sum_m x(m)e^{-j\frac{2\pi}{M}mm'}e^{-j\alpha m^2}.$$

The problem is how to determine the chirp-rate parameter $\alpha$ to obtain the best possible auto-focused radar image. Unfortunately, this cannot be performed in a simple manner. In the LPFT-based algorithm proposed in [22], a predefined set of chirp-rates is used, while the maximum likelihood (ML) procedure is employed to select the chirp-rate that produces the best radar image concentration. The complexity of this algorithm is proportional to the number of predefined chirp-rates [21]. On the other hand, the radar image can contain numerous targets, moving with various motion parameters, implying that various chirp-rate values are required for focusing all of them. Consequently, the predefined set should be large enough (thousands of components). The computational burden is additionally increased when the search for the third-order phase parameters is performed.

The PHAF is obtained as a modification of the polynomial phase transform (PPT), [23], and multi-lag high-order ambiguity function (ml-HAF) [24]. In order to overcome the PPT estimation ambiguity when multicomponent PPSs with the same highest-order phase coefficients are considered, the PHAF is introduced in [15]. Multicomponent PPSs with the same highest-order phase coefficients appear in the SAR systems, when two or more targets have the same motion parameters.

The multi-lag high-order instantaneous moments (ml-HIMs) of the signal $x(m)$ (7), are defined as [15]:

$$\begin{aligned} x_1(m) &= x(m) \\ x_2(m;\boldsymbol{\tau}_1) &= x_1(m+\boldsymbol{\tau}_1)x_1^*(m-\boldsymbol{\tau}_1) \\ x_3(m;\boldsymbol{\tau}_2) &= x_2(m+\boldsymbol{\tau}_2;\boldsymbol{\tau}_1)x_2^*(m-\boldsymbol{\tau}_2;\boldsymbol{\tau}_1) \\ &\cdots \\ x_P(m;\boldsymbol{\tau}_{P-1}) &= x_{P-1}(m+\boldsymbol{\tau}_{P-1};\boldsymbol{\tau}_{P-2}) \\ &\quad \times x_{P-1}^*(m-\boldsymbol{\tau}_{P-1};\boldsymbol{\tau}_{P-2}) \end{aligned} \tag{8}$$

where $\boldsymbol{\tau}_i = [\tau_1, \tau_2, \cdots, \tau_i]$, $i = 1, ..., P-1$, are the sets of used time lags.

The ml-HAF is defined as the FT of the ml-HIM:

$$X_P(f;\boldsymbol{\tau}_{P-1}) = \sum_{m=0}^{M} x_P(m;\boldsymbol{\tau}_{P-1})e^{-j2\pi fm}. \tag{9}$$

When the analyzed signal is a monocomponent $P$th order PPS (7), the $P$th order ml-HIM is a complex sinusoid with the frequency $f = 2^{P-1}P!\Pi_{k=1}^{P-1}\tau_k\alpha_P$, [15]. Coefficient $\alpha_P$ can be therefore estimated by searching for the position of maximum in the ml-HAF. If we dechirp the analyzed signal by using the estimated value, the resulting signal would be the $(P-1)$th order PPS. This procedure can be repeated in order to estimate lower-order phase coefficients. In case of $K$ moving targets, the corresponding radar signal is composed of $K$ components that are generally the $P$th order PPSs. The $P$th-order ml-HIM is then composed of $K$ complex sinusoids representing auto-terms. In this case, there is a number of cross-terms in the ml-HIM, which are, in general, the $P$th-order PPSs [15]. Specially, when the highest-order phase coefficients of some signal components are equal, the corresponding cross-terms are complex sinusoids [15], implying that some of the peaks in the ml-HAF correspond to the cross-terms. Consequently, the phase coefficients estimated by using maxima in the ml-HAF are ambiguous. The peak corresponding to a cross-term can be detected as a maximum leading to the inaccurate estimation of the PPS's coefficients.

The influence of cross-terms can be considerably attenuated by using the PHAF [15]. The PHAF is based on the fact that, unlike the cross-terms, the auto-terms are at frequencies proportional to the product of time lags used for the calculation of the ml-HAF. Therefore, in the PHAF, $L$ sets of time lags are used:

$$\mathbf{T}_{P-1}^{L} = [\boldsymbol{\tau}_{P-1}^{(1)}, \boldsymbol{\tau}_{P-1}^{(2)}, \cdots, \boldsymbol{\tau}_{P-1}^{(L)}], \tag{10}$$

where $\boldsymbol{\tau}_{P-1}^{(l)} = [\tau_1^{(l)}, \tau_2^{(l)}, \cdots, \tau_{P-1}^{(l)}]$ and $l = 1, ..., L$. The PHAF is defined as [15]:

$$X_P^L(f, \mathbf{T}_{P-1}^{L}) = \prod_{l=1}^{L} X_P(\beta^{(l)}f, \boldsymbol{\tau}_{\mathbf{P-1}}^{(\mathbf{l})}), \tag{11}$$

with the scaling coefficient equal to:

$$\beta^{(l)} = \frac{\prod_{k=1}^{P-1}\tau_k^{(l)}}{\prod_{k=1}^{P-1}\tau_k^{(1)}}. \tag{12}$$

In the PHAF, (11), the auto-terms are enhanced, since they are at the same positions in

the scaled frequency for each ml-HAF, whereas the cross-terms are attenuated, since they are not aligned in the ml-HAFs obtained after scaling over frequency.

### *B. The PHAF in SAR imaging*

We propose here a modification of the LPFT-based algorithm presented in [22]. When one or more unfocused targets are detected in a range bin, phase parameters of the corresponding signals are estimated by using the second and third-order PHAF. In each algorithm iteration, the phase parameters of one target (or couple of targets with the same or similar motion parameters) are estimated. The error of the third-order coefficient estimation propagates to the estimation of the second-order coefficient [15]. In order to overcome this problem, the fine search is performed around the coarse estimate obtained by using the PHAF. The third-order LPFT is used in the fine search. The search is performed in the interval of two frequency bins from each side of the frequency that the coarse estimate corresponds to. In our simulations, a set of 41 values is shown to be enough to provide high concentration of targets with various motion parameters. Thus, by using the PHAF in the coarse search, the computational complexity of the LPFT-based algorithm is significantly decreased. Moreover, the effect of nonlinear frequency modulation of the signal is compensated. When the signal is linear FM, the estimated value of the third-order phase coefficient equals zero and it does not influence the concentration of the SAR image.

The proposed algorithm, with the PHAF-based parameters estimation, is composed of the following steps:

Step 1. Calculate the FT along "slow-time" of signal (6):

$$R(m') = \sum_m x(m) e^{-j2\pi m m'/M}.$$

Initialize the number of iterations and phase coefficients to zero, i.e. $q = 0$, $\hat{\alpha}_2^q = 0$, $\hat{\alpha}_3^q = 0$. Set $x_q(m) = x(m)$.

Step 2. If $x_q(m)$ has significant energy, i.e., $\sum_m |x_q(m)|^2 \geq \varepsilon'$, set $X_q(m') = R(m')$ if frequency $m'$ represents well focused component and $X_q(m') = 0$ otherwise. Update the non-focused components as $R(m') \leftarrow R(m') - X_q(m')$. In order to perform the proposed procedure for a small number of ranges, we use the threshold $\varepsilon'$ within $[0.2, 2]\%$ of entire signal energy for noiseless case. A component is recognized as possibly highly concentrated when the considered pixel $|X_q(m')|$ satisfies $|X_q(m')| \geq \varepsilon'' \max_{m'} |R(m')|$, where $\varepsilon'' \in [0, 1]$. In this manner, all components that exceed $\varepsilon'' \max_{m'} |R(m')|$ are assumed as candidates for highly concentrated components. In setting the value of parameter $\varepsilon''$ we have to consider two effects. The signal that corresponds to a nonfocused target is an FM one. It is spread along multiple frequency bins and its intensity is small. In addition, in practical cases, targets may have different (small) reflection coefficients. Therefore, in our examples, we use $\varepsilon'' = 0.1$ which represents a trade-off between these two effects. This relatively small threshold could generate fake components. They are removed by the condition that $X_q(m')$ is a local maximum, i.e., it should be significantly larger than the neighbor samples $|X_q(m')| \geq \kappa_r |X_q(m' \pm r)|$, $\kappa_r \geq 1$. Here, two neighbor frequency bins from each side are considered with $\kappa_1 = 2$ and $\kappa_2 = 4$.

Step 3. Remove the modulation obtained by dechirping performed in the $q-$th iteration, and calculate the signal corresponding to the updated nonfocused targets:

$$x_q(m) = IFT\{R(m') e^{j\hat{\alpha}_2^q m^2} e^{j\hat{\alpha}_3^q m^3}\}.$$

Step 4. Set $q = q+1$, calculate the third-order discrete PHAF $X_3^L(m', \mathbf{T}_2^L)$ of $x_q(m)$ and estimate the third-order phase coefficient as:

$$\hat{\alpha}_3^q = \arg\max_{m'} |X_3^L(m', \mathbf{T}_2^L)| / (2^2 3! \prod_{k=1}^{2} \tau_k^{(1)}). \tag{13}$$

Dechirp $x_q(m)$ by using estimated value $\hat{\alpha}_3^q$ as:

$$x'_q(m) = x_q(m) e^{-j2\pi\hat{\alpha}_3^q m^3}, \tag{14}$$

and calculate the second-order discrete PHAF $X_2^L(m', \mathbf{T}_1^L)$ of $x'_q(m)$. Estimate the initial value of the second-order phase coefficient

from $X_2^L(m', \mathbf{T}_1^L)$:

$$\alpha_2^q = \arg\max_{m'} |X_2^L(m', \mathbf{T}_1^L)|/(4\tau_1^{(1)}) \quad (15)$$

and form a set of the second-order phase coefficients, composed of a couple of tens of values around the estimated one:

$$\Lambda = [\alpha_2^q - 2/(M4\tau_1^{(1)}), \alpha_2^q + 2/(M4\tau_1^{(1)})], \quad (16)$$

where $M$ is the number of frequency samples.
Step 5. Calculate:

$$R_{\alpha_2^q}(m') = \sum_m x_q(m) e^{-j2\pi mm'/M - j\alpha_2^q m^2 - j\hat{\alpha}_3^q m^3}$$

for each value of $\alpha_2^q$ from the considered set $\Lambda$.
Step 6. Estimate the final second-order phase coefficient as:

$$(\hat{\alpha}_2^q, \hat{m}') = \arg\max_{(\alpha_2^q, m')} |R_{\alpha_2^q}(m')|,$$
$$R(m') = R_{\hat{\alpha}_2^q}(m'). \quad (17)$$

Go to Step 2.

The presented procedure is carried out for one range bin and it should be repeated for each range. In the case of a signal corrupted by additive white Gaussian noise, the threshold $\varepsilon'$ is set to $kN\hat{\sigma}^2$, where $N$ is the number of samples within one chirp, $\hat{\sigma}^2$ is the variance estimation obtained as in [22], while $k = 1.8$ is used in our simulations as in [21]. In the considered radar applications this threshold selection procedure produces accurate results. Depending on the signal type and noise environment, modified threshold selection can be required.

The concentration of a moving target, after focusing, depends on the accuracy of the estimated values $\hat{a}_2^q$ and $\hat{a}_3^q$. If the estimated values are equal to $\alpha_2^q$ and $\alpha_3^q$, respectively, the effect of the modulation will be completely removed. The resulting signal will be a complex sinusoid and the corresponding target will be highly concentrated in the SAR image. On the other hand, even in the noiseless case, the third-order phase coefficient estimated by using the PHAF can be biased [15]. This would additionally decrease the accuracy of the second-order phase coefficient estimation. The PHAF error propagation causes a shift of the maximum of the second-order PHAF (from which we obtain the initial estimation (15)) calculated for the dechirped signal. We assume that the maximum can be shifted at the most for two frequency bins from its true position. The fine search interval is then selected as two frequency bins around the frequency related to the coarse estimation obtained with the PHAF. This interval is divided into a set of equidistantly spaced chirp-rates providing higher resolution than the coarse search and therefore the improved accuracy. This leads to a higher concentration of target in the final SAR image (obtained as the LPFT calculated for the best possible match from $\Lambda$). In our simulations, we take 41 possible values within this interval. The obtained resolution is hence $d\alpha_2 = 4/40/(4M\tau_1^1)$, where $1/M$ is the normalized frequency bin. By the proposed techniques, the second-order phase coefficients can be refined within the range $[-0.5/(4\tau_1^1), 0.5/(4\tau_1^1))$. The LPFT algorithm [22] with the same resolution as the proposed one would require search over $10M$ elements.

### C. *Computational complexity of the proposed algorithm*

Let us now compare the complexity of the modified LPFT-based algorithm to the LPFT-based algorithm [22] and the adaptive SM [20]. The computational complexity of the adaptive SM and the LPFT-based algorithm is compared in [21]. The complexity of the adaptive SM is $O(3NM \log_2 MN)$ [21], whereas the computational complexity of the LPFT-based algorithm is $O(L_o NM \log_2 NM)$, where $L_o$ is the number of elements (chirp-rates) in $\Lambda$ [21]. This number of elements can be large (several hundreds or thousands), especially when targets have various motion parameters, what makes the LPFT-based algorithm computationally more demanding than the adaptive SM-based algorithm [21].

In the proposed algorithm we calculated the third and the second-order PHAF, and the third-order LPFT, as opposed to the second order LPFT calculated in [22]. Therefore, for performing a fair comparison, we firstly ana-

lyze the number of operations needed for the initial chirp-rate estimation from the PHAF and calculation of the second-order LPFT for each value from the set of chirp-rates formed using this estimation. The complexity of the second-order ml-HIM is of order $NM$ (8). For the calculation of each ml-HAF, additional $NM^2$ operations are needed. More precisely, due to the frequency scaling, the FFT algorithm cannot be used here. When only the second-order PHAF is implemented, multiplying three frequency-scaled ml-HAFs is shown to be sufficient to obtain well estimation of the initial chirp-rate. Thus, the overall computational complexity of the second-order PHAF is $O(3NM^2)$. The calculation complexity of the second-order LPFT is $O(L_1 NM \log_2 NM)$. Here, the number of elements (chirp-rates) in the set $\Lambda$ is denoted by $L_1$, and $L_1 \ll L_o$ (significantly smaller than search space in [22]). Therefore, the overall complexity of the proposed algorithm is significantly lower than that of the LPFT-based algorithm proposed in [22]. The complexity of the proposed algorithm is still higher than that of the adaptive SM [20], but in case of very close targets the proposed algorithm should be used in order to avoid the appearance of cross-terms, while preserving the good concentration. Moreover, the proposed algorithm is more robust to additive Gaussian noise than the adaptive SM.

When the target has cross-range acceleration, the resulting radar signal is a nonlinear FM signal along $m$ [5], [6]. The adaptive SM cannot completely concentrate such a signal [25]. The second-order LPFT may also fail to produce high concentration. Therefore, the third-order LPFT should be applied. When predefined sets of parameters are used, as in [22], a 2D search is required, which results in increased calculation complexity of order $O(L_o^2 NM \log_2 NM)$. It should be noted that the achieved concentration would be highly dependent on the predefined sets of phase coefficients. In the proposed algorithm, the calculation of the third-order LPFT requires additional $O(9NM^2)$ operations. Moreover, the proposed algorithm is fully automated since the fine search space is determined using the coarse estimate.

## IV. Examples

In this section, results obtained by the proposed algorithm are compared to those obtained by the 2D FT, the adaptive SM and the LPFT-based autofocusing algorithm with the predefined set of chirp-rates. In the first three examples we analyzed stationary targets and moving targets that produce linear FM signals. In the fourth and the fifth examples, the target motion that produces nonlinear FM signal is also considered.

*Example 1.* The simulation setup, composed of seven point scatterers, as in [21], is used. Targets No. 1, 3 and 4 are stationary, whereas the other targets are moving (No. 2, 5, 6 and 7). The motion parameters of the targets are given in Table I. The position of the targets can be described as $x_i(t) = x_{i0} + v_{xi}(0)t + \frac{1}{2}a_{xi}t^2$ and $y_i(t) = y_{i0} + v_{yi}(0)t + \frac{1}{2}a_{yi}t^2$. The radar signal reflected from all the point scatterers is obtained by using the superposition principle, that is, as the sum of individual echoes.

The CV 580 SAR system (C-band) parameters are used in this example. The radar operates at the frequency $f_0 = 5.3\,\mathrm{GHz}$. The bandwidth of linear FM signals is $B = 25\,\mathrm{MHz}$, the pulse repetition time is $T = 1/300\,\mathrm{s}$, with $M = 256$ pulses in one revisit and $N = 256$ samples within one pulse. The aircraft with the radar is moving along the $x$-axis with velocity $V = 130\,\mathrm{m/s}$. The radar's altitude is $h = 6\,\mathrm{km}$, while the radar's ground distance from the origin of the coordinate system connected to the targets is $10\,\mathrm{km}$ at $t = 0$.

The radar image obtained by using the 2D FT, as the standard tool for SAR imaging, is shown in Fig. 1a. The stationary targets are well focused, which is not the case for moving targets. By applying the adaptive SM-based procedure, Fig. 1b, the high concentration of moving targets is obtained, without defocusing the stationary ones. Cross-terms are also avoided, except in case of very close targets (No. 5 and 6). It can be seen from Figs. 1c-d, that the radar image obtained by using both versions of the LPFT-based algorithms (the one proposed in [22] and the modified version, we are proposing here) is highly concentrated. The stationary targets remain

TABLE I
MOTION PARAMETERS OF THE TARGETS USED IN EXAMPLE 1 AND EXAMPLE 3.

| Scatterer No. | 1 | 2 | 3 | 4 | 5 | 6 | 7 |
|---|---|---|---|---|---|---|---|
| $x_0$ [m] | 0 | 30 | -9 | 9 | -30 | -25.5 | 30 |
| $y_0$ [m] | 90 | 90 | 0 | 0 | -90 | -90 | -90 |
| $v_x$ $[\frac{\text{m}}{\text{s}}]$ | 0 | -9 | 0 | 0 | 12 | 13 | 0 |
| $v_y$ $[\frac{\text{m}}{\text{s}}]$ | 0 | -20 | 0 | 0 | 0 | 10 | 20 |
| $a_x$ $[\frac{\text{m}}{\text{s}^2}]$ | 0 | 2 | 0 | 0 | 0 | 0 | 0 |
| $a_y$ $[\frac{\text{m}}{\text{s}^2}]$ | 0 | 0 | 0 | 0 | 0 | 0 | 1 |

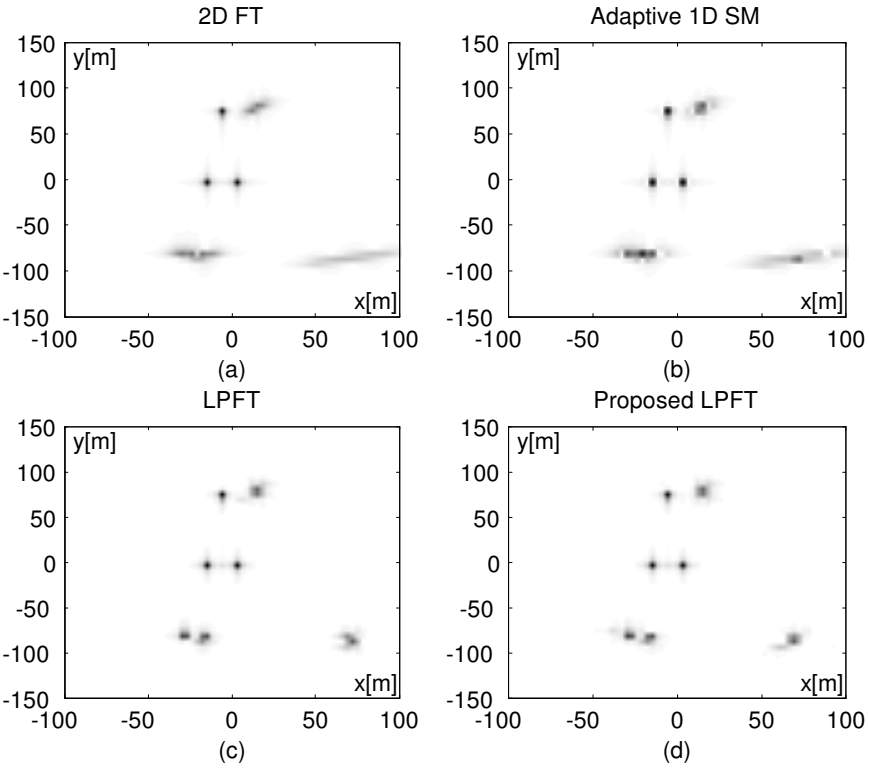


Fig. 1. Simulated SAR image of seven target points obtained by using: (a) 2D FT, (b) Adaptive S-method, (c) LPFT with predefined set of chirp rates, (d) Proposed LPFT.

focused and cross-terms are avoided, even between very close targets. In the algorithm proposed here, the calculational complexity is significantly decreased. In addition, its performance does not depend on the parameters of the target motion.

The polynomial phase order mismatching does not influence the performance of the proposed algorithm. To verify this, the third-order LPFT and PHAF are calculated, despite the fact that, for the used coherent integration time (CIT), the third-order term in the phase is small and can be neglected. Comparing to the standard second-order LPFT, the proposed procedure performs slightly better. If the second-order LPFT is applied in both algorithms, their performance will be the same. Here, the third-order phase terms of the sig-

nals corresponding to the moving targets are small, but they still slightly affect the focusing when there is more than one target in one range bin (No. 5, 6 and 7).

The time-lags used for the calculation of the third-order PHAF in the first three examples are $\boldsymbol{\tau}_2^{(1)} = [64, 42]$, $\boldsymbol{\tau}_2^{(2)} = [67, 45]$, $\boldsymbol{\tau}_2^{(3)} = [74, 48]$, $\boldsymbol{\tau}_2^{(4)} = [52, 30]$, $\boldsymbol{\tau}_2^{(5)} = [49, 52]$ and $\boldsymbol{\tau}_2^{(6)} = [61, 36]$. For the second-order PHAF, $\boldsymbol{\tau}_1^{(1)} = 64$, $\boldsymbol{\tau}_1^{(2)} = 67$ and $\boldsymbol{\tau}_1^{(3)} = 74$ should be used. The sets of time lags are chosen as recommended in [15], i.e., the optimal lag value for calculating the $p-$th order HAF is $\tau = M/P/2$, where $M$ is the number of available samples.

*Example 2.* In this example, we used the same radar setup as in the previous example. The illuminated scene is composed of two targets. The first target has fixed initial position $x_{01} = -30\,\mathrm{m}$, $y_{01} = -90\,\mathrm{m}$, and the constant cross-range velocity $v_{x1} = 12\,\mathrm{m/s}$. The cross-range velocity of the second target is $v_{x2} = 13\,\mathrm{m/s}$. It is at the same position as the first target along the range, while its initial position along the cross-range is changing from $x_{02} = -29.1\,\mathrm{m}$ to $x_{02} = 0\,\mathrm{m}$. For each initial position of the second target, the adaptive SM and the proposed algorithm are applied and the number of local maxima is counted. The calculations are performed along the cross-range for the fixed range that corresponds to the position of the maximum of the FT calculated along the "fast-time". The results are depicted in Fig. 2a, where the dotted line represents the number of local maxima in the adaptive SM, while the solid line represents the number of local maxima in the proposed algorithm. Since only two targets exist in the considered range, two maxima will be detected if the targets are separated and if there is no cross-term between them. Figure 2a shows that, even for very distant targets, more than two local maxima are detected in the adaptive SM. These additional maxima correspond to the side lobes. On the other hand, for the SAR imaging, only the dominant local maxima have significant influence on the image quality (see Fig. 1). Therefore, the experiment is repeated with the same setup, but now only dominant local maxima (higher than 20% of the global maximum for the observed range cell) are counted as potential targets. The number of detected targets, for both the adaptive SM (dotted line) and the proposed LPFT-based algorithm (solid line), is given in Fig. 2b, showing that the proposed algorithm has better resolution than the adaptive SM.

*Example 3.* Here, we use the same setup as in Example 1. The radar signal is embedded in the Gaussian white additive noise with the standard deviation $\sigma = 18$, as in [21]. The proposed algorithm (Fig. 3d), even in the presence of noise, performs as good as the LPFT-based algorithm with the predefined set of chirp-rates (Fig. 3c). It produces well focused radar image without cross-terms. The presence of noise decreases the concentration of the targets in the adaptive SM (Fig. 3b), comparing to the noiseless case (Fig. 1b). As a consequence, the fast moving target (No. 7) is almost invisible compared to the other, well focused targets.

From Fig. 3, it can be seen that both LPFT-based algorithms reduce the level of noise comparing to the 2D FT and the adaptive SM. The noise is statistically distributed in the LPFT in the same manner as in the FT. However, for the same distribution of noise, the LPFT produces better concentration of the targets. Obtained results are as expected. Namely, in these algorithms, only the well focused parts of the initial radar image (Fig. 3a) that correspond to the stationary targets, and the parts of the image determined as moving targets and additionally focused by applying the LPFT, appear in the resulting radar image. The "intensities" of other parts of the image are set to zero. Moreover, a relatively small portion of the radar image is related to the targets, while the noise is spread along the entire radar image. Thus, a significant portion of noise is discarded by this algorithm.

*Example 4.* In order to illustrate the effectiveness of the proposed algorithm when the target motion results in the third-order polynomial phase of the corresponding signal, we use CIT, $T = 3.4133\,\mathrm{s}$, that is four times longer than one used in the previous examples. The number of samples within one chirp

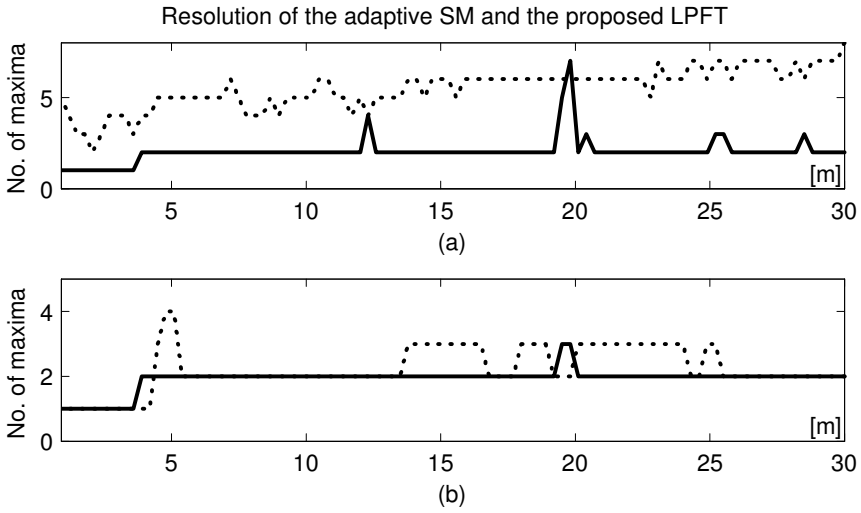


Fig. 2. (a) Number of detected local maxima (targets) after the adaptive SM (dotted line) and the proposed LPFT-based algorithm (solid line) are applied. (b) Number of detected dominant local maxima (higher than 20% of global maximum for this range cell). The illuminated radar scene is composed of two targets with distance varying from 0.9 m to 30 m.

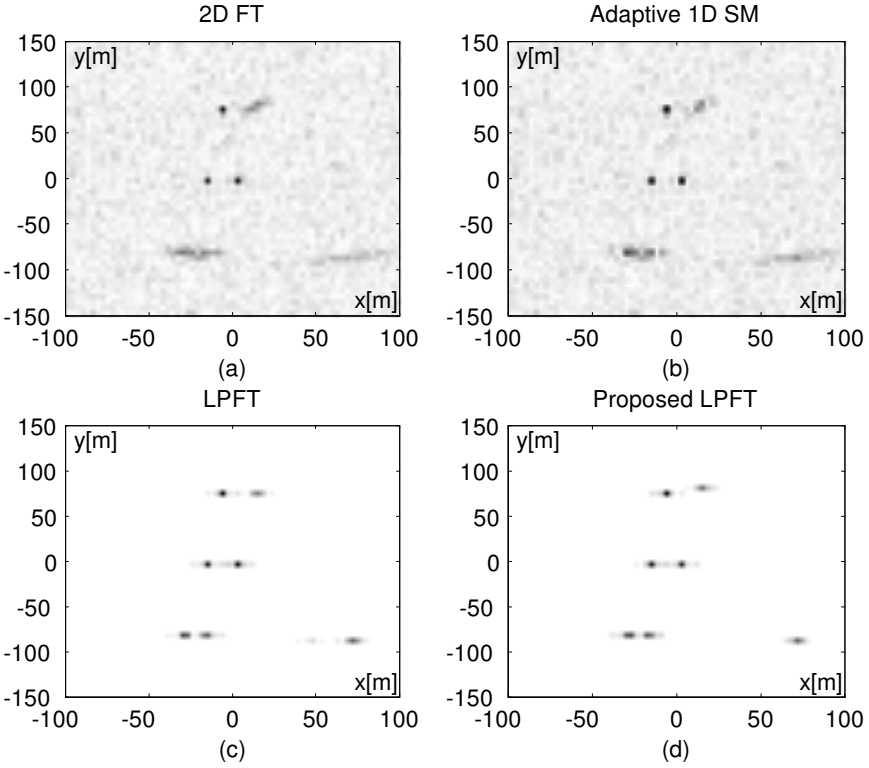


Fig. 3. Simulated SAR images of seven targets for radar signal embedded in white additive Gaussian noise obtained using (a) 2D FT, (b) Adaptive SM, (c) LPFT with the predefined set of chirp rates, (d) Proposed LPFT.

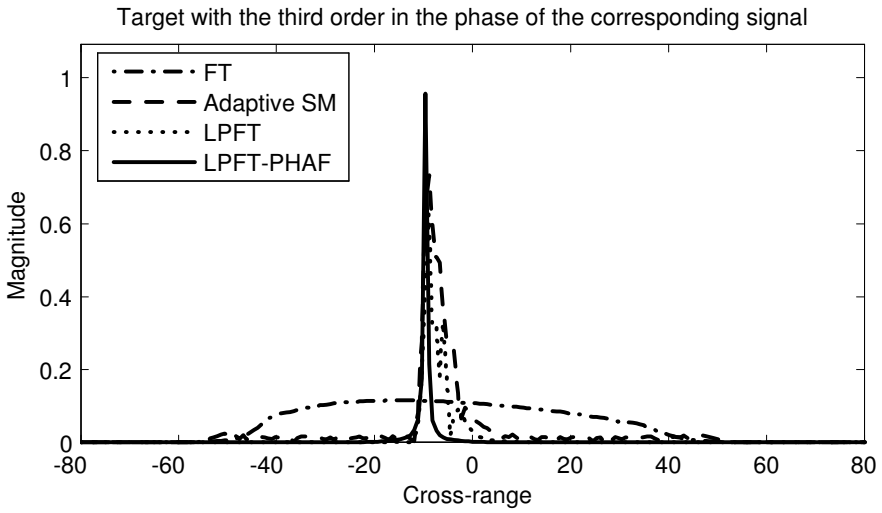


Fig. 4. Moving target, that results in the third-order phase, represented along the cross-range using the FT (dashdot line), the adaptive SM (dashed line), the second order LPFT with predefined set of parameters (dotted line) and the proposed third-order LPFT (solid line).

is $N = 1024$. The other parameters of the SAR system are the same as in the previous examples. The cross-range acceleration of a target results in nonlinear frequency modulation of the corresponding signal [5], [6]. In addition, this effect becomes significant only with the CIT comparable to the one used in [5] and [6]. Therefore, the radar scene is composed of one target with the initial position $(x_0, y_0) = (-30\,\mathrm{m}, -90\,\mathrm{m})$, the cross-range velocity $v_x = 10\,\mathrm{m/s}$ and the cross-range acceleration $a_x = 2\,\mathrm{m/s^2}$.

Figure 4 represents the target along the cross-range for the fixed range cell that corresponds to the target's position. In terms of peak concentration, the third-order LPFT outperforms other techniques. The adaptive SM and the second-order LPFT achieve better concentration than the FT, but the target is still smeared along the cross-range. The smearing in the second-order LPFT is due to the third-order term in the signal phase. The second-order LPFT compensates only the second-order phase term. The compensation of the third-order phase term can be performed by introducing the third-order in the LPFT. Then, two predefined sets of parameters will be used, implying a 2D search. Consequently, the LPFT would be highly computationally intensive. In addition, we have to know the expected cross-range acceleration interval in order to define the additional set of parameters. On the other hand, the adaptive SM is able to fully eliminate the linear frequency modulation of the signal [25], while the third-order term in the signal phase results in an unsatisfying concentration of the target.

For longer CIT, like the one used in this and the following example, the adaptive SM uses the threshold that equals 0.5% of the 2D FT based radar image. In addition, time-lags used for the calculation of the third-order PHAF are $\boldsymbol{\tau}_2^{(1)} = [256, 170]$, $\boldsymbol{\tau}_2^{(2)} = [268, 182]$, $\boldsymbol{\tau}_2^{(3)} = [296, 194]$, $\boldsymbol{\tau}_2^{(4)} = [208, 122]$, $\boldsymbol{\tau}_2^{(5)} = [196, 210]$, $\boldsymbol{\tau}_2^{(6)} = [244, 146]$.

*Example 5.* In this example, we use the same parameters of the SAR system as in the fourth example. Radar scene is composed of seven targets.

From the motion parameters given in Table II, it can be concluded that the target No. 7 can be accurately represented by the second-order PPS [20]. For targets No. 2, 5 and 6, the third-order phase term in the corresponding signal is significant and cannot be neglected [5], [6]. As expected, in the radar image ob-

TABLE II
MOTION PARAMETERS OF THE TARGETS USED IN EXAMPLE 5.

| Scatterer No. | 1 | 2 | 3 | 4 | 5 | 6 | 7 |
|---|---|---|---|---|---|---|---|
| $x_0$ [m] | 0 | 30 | -9 | 9 | -30 | -21 | 45 |
| $y_0$ [m] | 90 | 90 | 0 | 0 | -90 | -90 | -90 |
| $v_x$ $[\frac{\text{m}}{\text{s}}]$ | 0 | 5 | 0 | 0 | 6 | 8 | 10 |
| $v_y$ $[\frac{\text{m}}{\text{s}}]$ | 0 | 0 | 0 | 0 | 0 | 0 | 0 |
| $a_x$ $[\frac{\text{m}}{\text{s}^2}]$ | 0 | 2 | 0 | 0 | 1.8 | 2 | 0 |
| $a_y$ $[\frac{\text{m}}{\text{s}^2}]$ | 0 | 0 | 0 | 0 | 0 | 0 | 0 |

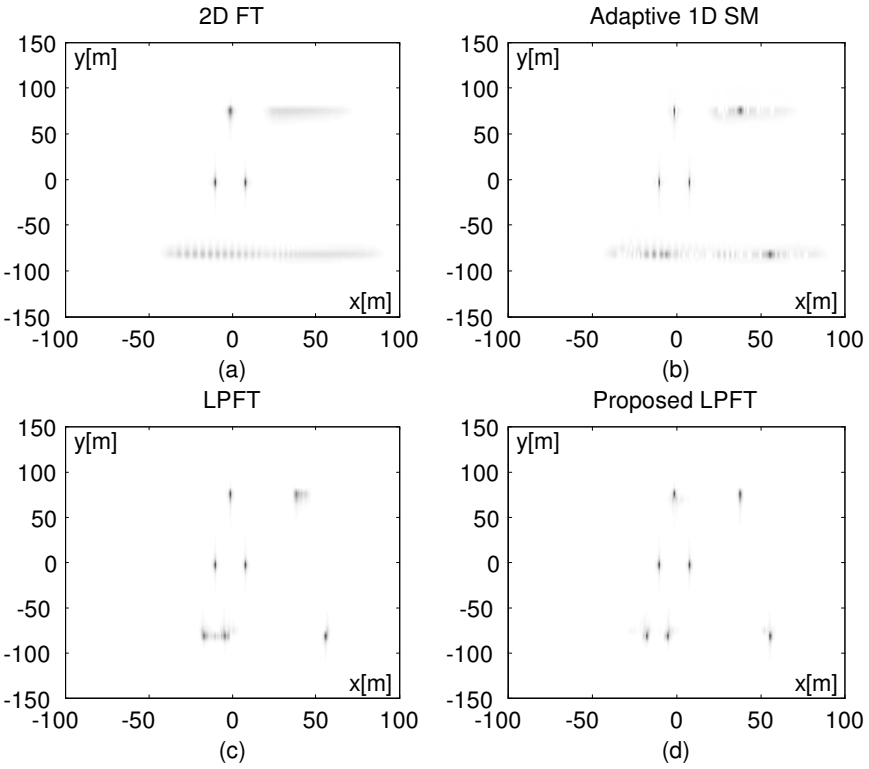


Fig. 5. Simulated SAR image of 7 target points obtained by using: (a) 2D FT, (b) Adaptive S-method, (c) LPFT with predefined set of chirp rates (d) Proposed LPFT.

tained by using the 2D FT, stationary targets are well focused (No. 1, 3 and 4), whereas the moving targets are smeared (Fig. 5a). After the adaptive SM is applied (Fig. 5b), the moving targets are better focused than in the 2D FT, but their concentration is not as high as that of the stationary targets. As a result of long CIT, the targets are spread along many cross-range bins in the 2D FT (Fig. 5a) and the summation in the adaptive SM stops before all side lobes become equal to zero. In addition, the SM is able to automatically compensate for even polynomial terms in the signal phase, while in case of odd coefficients the resulting radar image is still defocused (Fig. 4), [25]. The cross-terms appear between very close targets. The second-order LPFT-based algorithm, with the predefined set of chirp-

rates, produces high concentration of the target with constant cross-range velocity (No. 7). The stationary targets remain well focused in the resulting image. The targets with cross-range acceleration are better focused than in the adaptive SM, but not as well as the stationary ones, and those with the constant cross-range velocity (No. 1, 3, 4 and 7). Furthermore, the inability of the second-order LPFT to remove the third-order phase terms results in lower resolution between very close components (No. 5 and 6).

The proposed algorithm produces high concentration of all moving targets, without defocusing the stationary ones or inducing cross-terms (Fig. 5d). It is robust to the order mismatching since it produces high concentration of the target with the second-order PPS (No. 7). The value of the third-order phase coefficient estimated by the PHAF is equal to zero, and it does not influence the concentration of the target.

## V. Conclusions

We propose an LPFT-based algorithm for focusing SAR radar targets. The phase parameters are calculated by using the PHAF which yields significantly lower calculation complexity comparing to the existing algorithms. The PHAF error propagation is reduced by fine search around the coarse estimate obtained by the PHAF. The second-order phase coefficient, that provides the highest concentration, is determined and used for forming the final radar image. The fine search set contains small number of elements, and it is automatically adjusted, in each iteration, to the motion parameters of targets. The proposed algorithm therefore produces highly concentrated radar image, even in case of different motion parameters of targets, while preserving the fixed number of operations. When there is more than one target in the same range bin with different motion parameters, the proposed algorithm outperforms the PHAF already applied for the SAR imaging [12]. In addition, it outperforms the adaptive SM in case of close targets and in the presence of noise. The third-order PHAF is used here to obtain the high concentration of targets that result in third-order PPSs. For such targets, the adaptive SM is not able to achieve high concentration. Increasing the order of the LPFT in the algorithm proposed in [22] would cause a 2D search over the predefined sets of parameters, which would additionally increase its computational burden. The performance of the proposed algorithm is validated by examples.

## VI. Acknowledgement

This research was supported in part by the Ministry of Science and Education of Montenegro.

## References

[1] V. C. Chen, H. Ling: *Time-frequency transforms for radar imaging and signal analysis*, Artech House, Boston, USA, 2002.

[2] W. G. Carrara, R. S. Goodman, R. M. Majewski: *Spotlight synthetic aperture radar - signal processing algorithms*, Artech House, Norwood, 1995.

[3] S. Wong, E. Riseborough, G. Duff: "Experimental investigation on the distortion of ISAR images using different radar waveform", *Defence R&D Canada, Ottawa, Technical memorandum DRDC Ottawa,* TM 2003-196, Sept. 2003.

[4] S. R. DeGraaf: "SAR imaging via modern 2-D spectral estimation methods", *IEEE Trans. Signal Processing*, vol. 7, no. 5, pp. 729-761, May 1998.

[5] J. J. Sharma, C. H. Gierull, and M. J. Collins: "Compensating the effects of target acceleration in dual-channel SAR-GMTI", *IEE Proc. of Radar, Sonar and Navigation*, vol. 153, no. 1, pp. 53-62, Feb. 2006.

[6] J. J. Sharma, C. H. Gierull, and M. J. Collins: "The influence of target acceleration on velocity estimation in dual-channel SAR-GMTI", *IEEE Trans. Geoscience and Remote Sensing*, vol. 44, no. 1, pp. 134–135, Jan. 2005.

[7] R. K. Raney: "Synthetic aperture imaging radar and moving targets", *IEEE Trans. Aerospace and Electronic Systems*, vol. 7, no. 3, pp. 499-505, May 1971.

[8] M. Kirscht: "Detection and imaging of arbitrarily moving targets with single-channel SAR", *IEE Proc. Radar, Sonar Navigation*, vol. 150, no. 1, pp. 7-11, Feb. 2003.

[9] H. L. Chan, T. S. Yeo: "Noniterative quality phase-gradient autofocus (QPGA) algorithm for spotlight SAR imagery", *IEEE Trans. Geoscience and Remote Sensing,* vol. 36, no. 5, Part 1, pp. 1531-1539, Sept. 1998.

[10] H. L. Chan, T. S. Yeo: "Comments on "Non-iterative quality phase-gradient autofocus (QPGA) algorithm for spotlight SAR imagery"", *IEEE Trans. Geoscience and Remote Sensing,* vol. 40, no. 11, p. 2517, Nov. 2002.

[11] D. E. Wahl, P. H. Eichel, D. C. Ghiglia, C. V. Jakowatz Jr: "Phase gradient autofocus-a robust tool for high resolution SAR phase correction",

*IEEE Trans. Aerospace and Electronic Systems*, vol. 30, no. 3, pp. 827 - 835, July 1994.

[12] S. Barbarossa, A. Scaglione: "Autofocusing of SAR images based on the product high-order ambiguity function", *IEE Proc. Radar, Sonar Navigation*, vol. 145, no. 5, pp. 269 - 273, Oct 1998.

[13] A. Moreira: "Real-time synthetic aperture radar (SAR) processing with a new subaperture approach", *IEEE Trans. Geoscience and Remote Sensing*, vol. 30, no. 4, pp. 714-722, July 1992.

[14] A. Moreira, J. Mittermayer, R. Scheiber: "Extended chirp scaling algorithm for air- and spaceborne SAR dataprocessing in stripmap and ScanSAR imaging modes", *IEEE Trans. Geoscience and Remote Sensing*, vol. 34, no. 5, pp. 1123-1136, Sep. 1996.

[15] S. Barbarossa, A. Scaglione, G. B. Giannakis: "Product high-order ambiguity function for multicomponent polynomial phase signal modeling", *IEEE Trans. Signal Process.*, vol. 46, no.3, pp. 691–708, Mar. 1998.

[16] T. Sparr, B. Krane: "Micro-Doppler analysis of vibrating targets in SAR", *IEE Proc. Radar Sonar Navig.*, vol 150, no. 4, pp. 277-283, Aug. 2003.

[17] Y. Wang, H. Ling, V. C. Chen: "ISAR motion compensation via adaptive joint time-frequency techniques", *IEEE Trans. Aerospace and Electronics Systems*, vol. 34, no. 2, pp. 670–677, April 1988.

[18] V. N. Ivanović, M. Daković, LJ. Stanković: "Performance of quadratic time-frequency distributions as instantaneous frequency estimators", *IEEE Trans.on Signal Processing*, vol. 51, no.1, pp. 77-89, Jan. 2003.

[19] B. Boashash: "Estimating and interpreting the instantaneous frequency of a signal Part 1", *IEEE Proc.*, vol. 80, no. 4, pp. 519-538, April 1992.

[20] LJ. Stanković, T. Thayaparan, V. Popović, I. Djurović and M. Daković: "Adaptive S-method for SAR/ISAR imaging", *EURASIP Journal on Advances in Signal Processing*, vol. 2008, Article ID 593216, 10 pages, 2008. doi:10.1155/2008/593216.

[21] I. Djurović, LJ. Stanković, T. Thayaparan, V. Popović, M. Daković: "Time-frequency analysis for SAR and ISAR imaging", in *GeoSpatial Visual Analytics*, Springer Netherlands, pp. 113-127, 2009.

[22] I. Djurović, T. Thayaparan, LJ. Stanković: "SAR imaging of moving targets using polynomial Fourier transform", *IET Signal Processing*, vol. 2, no. 3, pp. 237 - 246, Sept. 2008.

[23] S. Peleg, B. Porat: "Estimation and classification of polynomial phase signals", *IEEE Trans. on Inf. Theory*, vol. 37, pp. 422–430, Mar. 1991.

[24] S. Barbarossa, "Detection and estimation of the instantaneous frequency of polynomial-phase signals by multilinear time-frequency representations", in Proc. *IEEE SP Workshop on Higher Order Statistics*, South Lake Tahoe, CA, pp.168-172, June 1993.

[25] T. Thayaparan, LJ. Stanković, C. Wernik, M. Daković: "Real-time motion compensation, image formation and image enhancement of moving targets in ISAR and SAR using S-method based approach", *IET Signal Processing*, vol. 2, no. 3, pp. 247-264, Aug. 2008.